Zeitschrift: Schweizerische mineralogische und petrographische Mitteilungen = Bulletin suisse de minéralogie et pétrographie

Band: 72 (1992)

Heft: 2

Artikel: Neogene and Quaternary volcanism on Spitsbergen : the revival of an Arctic Hot Spot

Autor: Tuchschmid, Martin / Spillmann, Peter

DOI: https://doi.org/10.5169/seals-54911

SCHWEIZ. MINERAL. PETROGR. MITT. 72, 251–270, 1992

Neogene and Quaternary volcanism on Spitsbergen – the revival of an Arctic Hot Spot

by *Martin Tuchschmid* and *Peter Spillmann*[1]

Abstract

Late Cenozoic volcanic activity on Spitsbergen (Svalbard Archipelago) is of particular interest as it represents the only known late Cenozoic continental volcanism which is related to the constructive Eurasian-American plate boundary. A subdivision of the volcanic activity in a Neogene and a Pleistocene episode can be made by their structural settings. To contrast these distinct volcanic phases we present volcanological and petrographical observations, as well as analyses of whole rock and mineral chemistry on Neogene and Pleistocene lavas and pyroclastic rocks from NW-Spitsbergen. The lavas of the voluminous, purely effusive Neogene volcanism have subalkaline olivine tholeiitic and weakly alkaline olivine basaltic compositions. Petrologic characteristics of the Neogene lavas require upper crustal magma chambers as the sites of olivine fractionation and mixing of mantle derived magma batches, which most likely originated in a spinel-lherzolitic source contaminated by deep mantle melts. The products of the effusive and explosive Pleistocene volcanism have primitive, basanitic compositions and include large amounts of upper mantle xenoliths. Basanite evolution from parental melts was dominated by higher pressure (10–15 kb) crystallization, little olivine fractionation and contamination with upper mantle xenoliths. REE geochemistry of the basanites suggests that they were generated in a garnet-lherzolitic source. A mantle plume model is proposed for the evolution of late Cenozoic magmatism on Spitsbergen, which is associated to coeval off-shore magmatism north of Spitsbergen. A renewed activity of the pre-Oligocene Yermak Hot Spot since Miocene times is confirmed by the proposed model.

Keywords: Volcanic rocks, geochemistry, xenolith, mantle plume, hot spot, Spitsbergen, Late Cenozoic.

1. Introduction

Spitsbergen is the largest island (39 000 km^2) of the Svalbard Archipelago located in the Arctic between latitudes 74°N and 81°N, and longitudes 10°E and 35°E. The group of islands is situated at the northwesternmost edge of the continental Barents shelf 1000 km north of Norway (Fig. 1). A narrow ocean basin west of Svalbard joins the oceanic Greenland and Eurasian basins. This so called "Spitsbergen Transform Zone" was established during continental fragmentation of Laurasia in Cenozoic times (HARLAND, 1969; CRANE et al., 1982; HANISCH, 1984). It now represents an array of short ridge segments, connected by transform faults, which links the Knipovich Ridge to the south with the Nansen Ridge to the north (Fig. 1). Magnetic and bathymetric data give evidence for a former mantle upwelling zone at the southern end of the Nansen Ridge, the "Yermak Hot Spot" (JACKSON et al., 1984; FEDEN et al., 1979). Morphologic and geophysical manifestations of this hot spot, active in the Paleocene and Eocene, are found at two aseismic ridges: the Yermak Plateau and the Morris Jesup Rise, which are separated by the Nansen Ridge (Fig. 1). Geophysical evidence on the Yermak Plateau and at the Nansen Ridge suggests a reactivation of the hot spot in the Miocene (FEDEN et al., 1979; CRANE et al., 1982).

[1] Institut für Mineralogie und Petrographie, Swiss Federal Institute of Technology, ETH-Zentrum, CH-8092 Zürich.

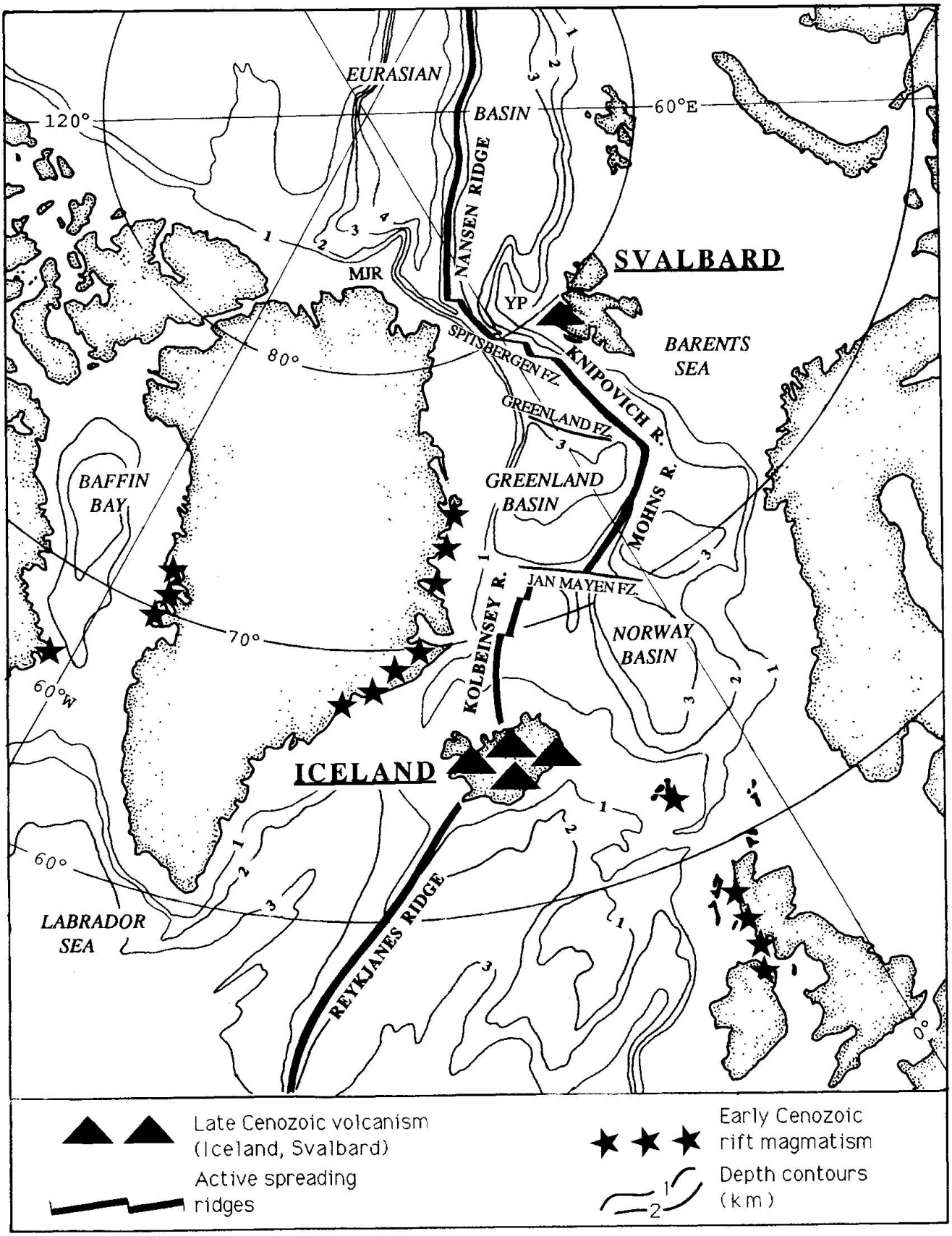

Fig. 1 Physiographical map of the North Atlantic and the Arctic (after HARLAND, 1969; VOGT et al., 1982), (MJR: Morris Jesup Rise; YP: Yermak Plateau).

Continental fragmentation in the northern North Atlantic and in the Eurasian Basin started in the Paleocene (TALWANI and ELDHOLM, 1977; FEDEN et al., 1979) and was accompanied by widespread rift magmatism (HARLAND, 1969). Numerous regions with Paleocene magmatism are known from the passive continental margins of the northern North Atlantic (e.g. Skaergaard Intrusive Complex, British Tertiary Volcanic Province; for an overview see DICKIN, 1988). Remnants of this magmatic activity have not been observed on Svalbard. In the Neogene and Quaternary, magmatism in the North Atlantic and the Arctic was restricted to spreading ridges. An exception is the continental volcanism in NW-Spitsbergen (Fig. 1), where two distinct phases of basic volcanism occurred in Neogene and Pleistocene times. The volcanic centres are bound to N-S-trending faults which project towards the Yermak Plateau and parallel the Spitsbergen Transform Zone. This late Cenozoic continental volcanism is unique as it is the only known in the Arctic region and provides important information about the nature of the upper mantle and lower crust in this region. The Pleistocene volcanoes are known as one of the world's richest occurrence of mantle xenoliths (GJELSVIK, 1963; AMUNDSEN et al., 1987a, 1987b).

Previous investigations have focused either on the Neogene volcanism (HOEL and HOLTEDAHL, 1911; PRESTVIK, 1977; HAGEN, 1988) or on the Quaternary volcanism in NW-Spitsbergen (GJELSVIK, 1963; SKJELKVÅLE et al., 1989). Recently, studies on mantle xenoliths from Quaternary volcanics (FURNES et al., 1986; AMUNDSEN, 1987b; AMUNDSEN et al., 1987a, 1987b) and petrological modelling of the Neogene volcanic activity have been carried out (HAGEN, 1988). Our investigation presents new petrographical and chemical data on both phases of volcanism in NW-Spitsbergen and discusses the petrologic evolution of the Neogene and Pleistocene volcanics. Considering our results and published data on the petrologic characteristics of the upper mantle below Spitsbergen as well as the geologic and plate tectonic evolution of Spitsbergen and its surrounding areas, a qualitative model for the Neogene and Quaternary tectono-magmatic history of Spitsbergen is proposed.

2. Geologic setting

A comprehensive discussion of the geology of Svalbard is given by BIRKENMAJER (1981). The crystalline basement rocks on Svalbard, predominantly exposed in northern and western Svalbard (Fig. 2), consist of variably metamorphosed sedimentary and volcanic series of Proterozoic to Paleozoic age (Hecla Hoek Fm., GEE and HJELLE, 1966; HJELLE, 1966; HJELLE and OHTA, 1974). Metamorphism and deformation is of Caledonian age and was followed by the emplacement of post-tectonic granitic rocks (GAYER et al., 1966). The end of Caledonian diastrophism at the Silurian/Devonian boundary was followed by uplift and erosion of the orogenic belt. Molasse-type sediments (Old Red Sandstones, FRIEND and MOODY-STUART, 1972) were deposited and are now present in narrow syn- or postsedimentary graben structures (Fig. 2). Late Devonian tectonism caused folding and faulting of the Old Red formation (HARLAND et al., 1974; LAMAR et al., 1986). Predominantly clastic marine to deltaic sedimentation in the Upper Paleozoic marks the onset of the post-Caledonian platform sequence on Svalbard (STEEL and WORSLEY, 1984). A stable marine platform, established in Mesozoic times, witnessed a period of tectonic stability. The intrusion of dolerites into Upper Jurassic and Lower Cretaceous strata (WEIGAND and TESTA, 1982) in central and eastern Svalbard (Fig. 2) indicates renewed tectonic activity at the end of the Mesozoic (STEEL and WORSLEY, 1984).

Two phases of tectonic activity are distinguished in the Tertiary of Svalbard, both closely related to the plate-tectonic evolution of North Atlantic and Arctic regions:

1. The breakup of Laurasia along spreading centres in the North Atlantic and in the Labrador Sea as well as along the Nansen Ridge in the Eurasian Basin (Fig. 1) caused a transpressive tectonic regime on Svalbard during the Paleocene and Eocene (HARLAND, 1969; TALWANI and ELDHOLM, 1977). As a consequence Spitsbergen was subjected to strong deformation which resulted in the formation of a thrust and fold belt along the west coast of Spitsbergen (Fig. 2). Paleogene sediments were deposited into syn- to post-tectonic foreland basins in southern and western Spitsbergen (BIRKENMAJER, 1981). There is a controversy about the exact timing of this so-called "West Spitsbergen orogeny" (HARLAND, 1969; HANISCH, 1984).

2. Since the Oligocene the tectonic regime has changed to transtensive, due to a change in plate motion between Greenland and Eurasia induced by the end of spreading in the Labrador Sea (KRISTOFFERSON and TALWANI, 1977). This situation led to increased spreading along the Knipovich Ridge (ELDHOLM and TALWANI, 1977). The formation or reactivation of N/S-striking normal faults (Fig. 2) is characteristic for this period on Spitsbergen (STEEL and WORSLEY, 1984). A post-

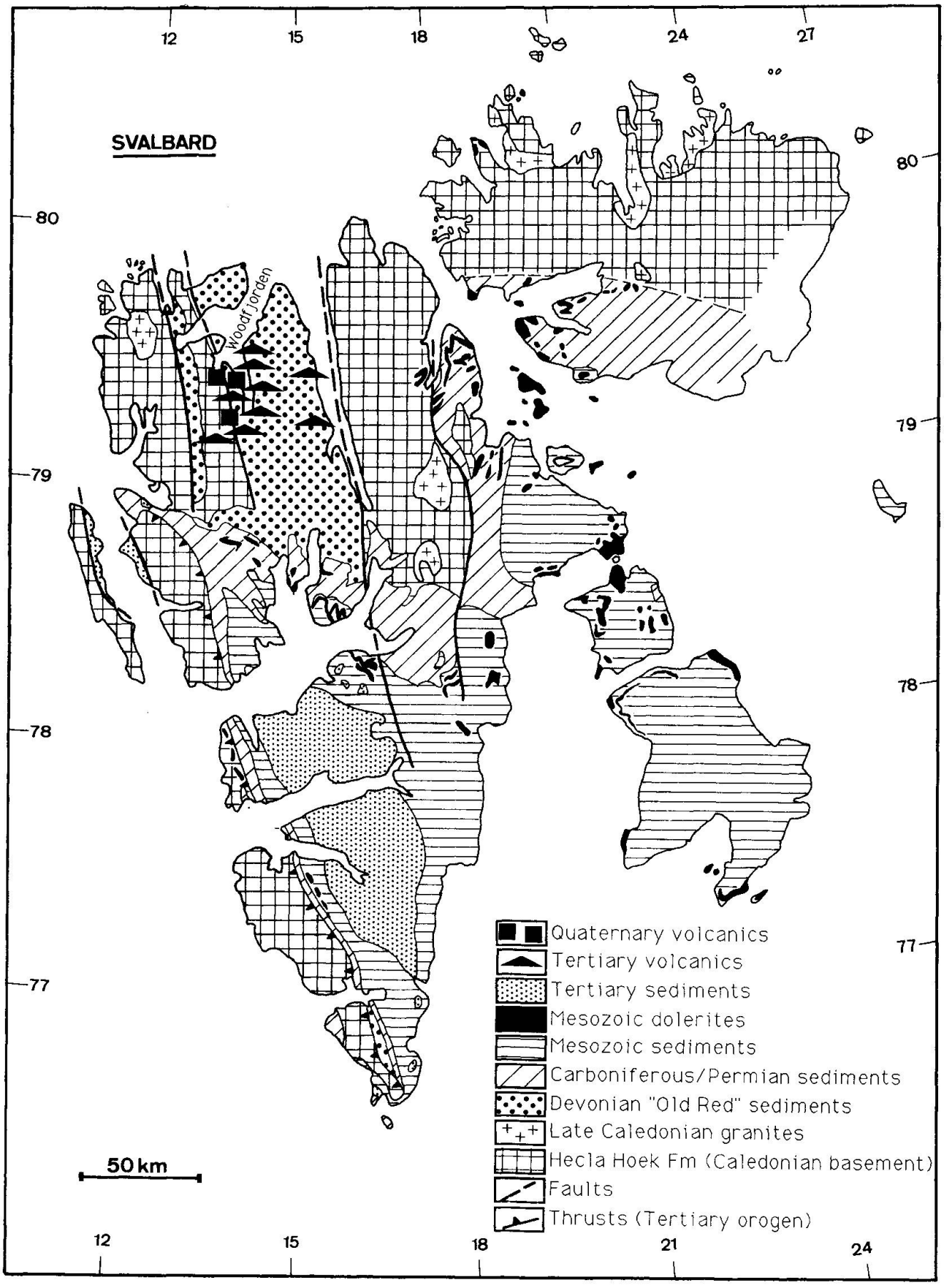

Fig. 2 Geological map of Svalbard (redrawn after HARLAND, 1969).

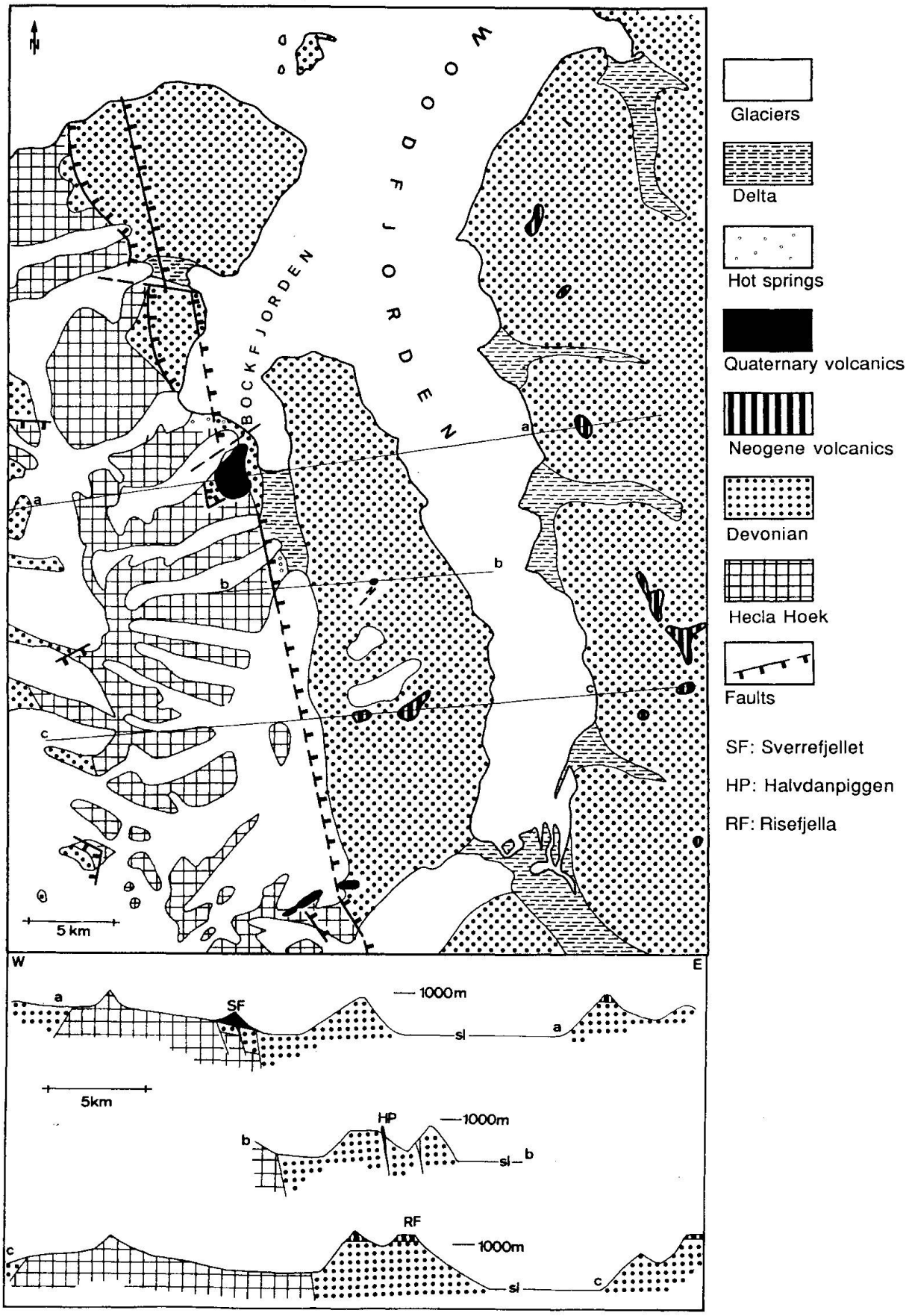

Fig. 3 Geological map of the Bockfjorden and Woodfjorden area (after SKJELKVÅLE et al., 1989; HJELLE and LAURITZEN, 1982; GJELSVIK, 1979).

orogenic peneplanation followed by uplift (average 1000 m) could be the cause for the uniformity of summit heights on Spitsbergen (HARLAND, 1969). In NW-Spitsbergen, in the region of Woodfjorden, many mountain peaks are capped by remnants of basaltic lava flow successions (Figs 2 and 3) (HOEL, 1914), erupted on the Late Tertiary peneplain prior to regional uplift. PRESTVIK (1977) gives K/Ar-ages of 10 to 12 m.y. for these basalts.

The Quaternary sediments of the Svalbard archipelago consist of Pleistocene and Holocene glacial deposits and Holocene raised marine beaches (SALVIGSEN and ÖSTERHOLM, 1982). Basanitic melts were extruded onto the Pleistocene, ice-sculptured landscape at the three known centres of Early Quaternary volcanism in NW-Spitsbergen (Figs 2 and 3) (HOEL and HOLTEDAHL, 1911; SKJELKVÅLE et al., 1989): Sverrefjellet (a Late Pleistocene stratovolcano), Halvdanpiggen (an Early Pleistocene volcanic neck) and an eruptive centre of uncertain age at Sigurdfjellet. The Pleistocene volcanic rocks are very rich in xenolithic material of upper mantle and crustal origin, discussed in detail by AMUNDSEN (1987a) and AMUNDSEN et al. (1987a, 1987b). Recent hydrothermal activity is indicated by the occurrence of hot springs (Fig. 3).

3. Analytical techniques

Mineral compositions of Neogene and Pleistocene volcanic rocks were analyzed by using a Cameca SX50 electron microprobe. The analyses were carried out by wavelength dispersive systems, using an accelerating voltage of 15 kV and a beam current of 20 nA. The selected X-ray lines, diffraction crystals, analyzed X-ray wavelengths as well as standard materials and their compositions are listed in table 1. Acquisition time was 10 sec. Peak intensities were corrected for deadtime and background. Matrix corrections were made using the ZAF technique. Detection limits for all analyzed elements were approximately 0.03 wt% oxide compound. Relative 2σ-accuracies have been estimated to be 1–2%, 2–5% and 5–10% for oxide compounds of more than 5 wt%, 1–5 wt% and less than 1 wt%, respectively.

For bulk chemical analyses the volcanic samples were ground in a wolfram-carbide mill. Before grinding, Quaternary volcanic samples were broken and fragments were handpicked to make them visually free of xenolithic material.

Major element whole rock compositions were determined by X-ray fluorescence analysis (XRF) of glass beads with a Philips PW1450 sequential spectrometer at the EMPA (Eidgenössische Materialprüfungsanstalt, Dübendorf); the glass beads were fused in gold-platinum pans at 1150 °C from rock powders ignited at 1050 °C and dried Lithium-Tetraborate (1 : 5 ratio). Net intensities were corrected for drift, background, and matrix effects (DIETRICH et al., 1976). FeO contents were analyzed spectrophotometrically (AYRANCI, 1977). Fe_2O_3 and H_2O contents were recalculated from analyzed Fe_2O_3 (total) and FeO contents and loss of ignition. Trace element bulk compositions were determined by XRF of powder samples, using the synthetic background method (NISBET et al., 1979). The correction and calibration procedures of major and trace elements by FORTRAN programs are described in detail by REUSSER (1987). USGS reference rock samples were used for calibration. Detection limits were 3 to 6 ppm for most trace elements. Relative 2σ-accuracies were 2–3% at 1000 ppm, 5–10% at 100 ppm, and 10–20% at 10 ppm for trace elements, and 2–3% for major elements.

REE, U, Th and Hf bulk contents were determined by instrumental neutron activation analyses (INAA) at the PSI (Paul Scherrer Institut, Würenlingen) and by inductively coupled plasma mass spectrometry (ICP-MS) at the EMPA. For INAA 100 mg of rock powder were put in polyethylene containers and irradiated by thermal neutrons. The Gamma-spectra (up to 500 keV with 0.25 keV/channel) were analyzed with a planar intrinsic Ge-detector after 7, 20 and 30 days (WYTTENBACH et al., 1983). The spectra were evaluated by using the program JANE developed by SCHUBIGER et al. (1978). AAS standard solutions (ALFA) were used for calibration. The analyzed elements were La, Ce, Nd, Sm, Eu, Tb, Yb, Lu, U, Hf and Th. Relative 1σ-accuracies were estimated to be 1–2% for LREE and Hf, 4–7% for HREE and Th, and 10–20% for U. For ICP-MS 100 mg of rock powder were dissolved with 1 ml HF and 4 ml HNO_3 in teflon containers. Dissolution took about 45 minutes in a microwave apparatus (MLS 1200) at increasing power up to 400 W. The dissolved samples were diluted to 100 ml with de-ionized water. The solutions were analyzed on a ELAN 5000 (Perkin-Elmer Sciex) apparatus with a 40 MHz (free running) generator and a cross flow nebulizer. Gas flows were 15 l/min (plasma), 0.8 l/min (auxiliary) and 0.9 l/min (nebulizer). Sample uptake rate was 1 ml/min. Specpure standard solutions were used for calibration. Rh was used as an internal standard for drift corrections. All naturally occurring REE (except Gd) plus U and Hf were analyzed. Relative 1σ-accuracies were estimated to be 1–3% for REE and 2–4% for U and Hf. INAA and ICP-MS

Tab. 1 Experimental array of electron microprobe analyses.

element	diffraction crystal	emission line	wavelength [A]	standard material	concentration [wt% of oxide]
Ca (II)	PET	Kα1	3.35839	Wollastonite	48.21
K (I)	PET	Kα1	3.74140	Orthoclase	14.92
Fe (III)	LIF	Kα1	1.93604	Haematite	99.96
Na (I)	TAP	Kα1	11.91010	Aegirine-augite	13.32
Si (IV)	TAP	Kα1	7.12542	Quartz	100.00
Ti (IV)	PET	Kα1	2.74851	Rutile (synth.)	100.00
Cr (III)	PET	Kα1	2.28970	Eskolaite (synth.)	99.66
Mn (II)	LIF	Kα1	2.10182	Tephroite (synth.)	70.10
Mg (II)	TAP	Kα1	9.89000	Periclase (synth.)	100.00
Al (III)	TAP	Kα1	8.33934	Corundum	99.00
Ni (II)	LIF	Kα1	1.65791	Ni-Oxide (synth.)	100.00

techniques were checked by analysing international rock standards (BCR-1, BHVO-1).

4. Results

4.1. VOLCANOLOGY

4.1.1. Neogene volcanic activity

The Neogene volcanic rocks studied in this work occur at Risefjella in the Woodfjord area (Fig. 3) and belong to a 150 m thick succession of flat-lying, basaltic flows. The dense to highly vesicular, subaerial lava flows range in thickness from 3 to 5 meters, some of which show columnar jointing. In many flows clear evidence for magma mixing (rods, irregular bands and small pipes of lighter lava in a darker lava or vice versa) has been observed (Fig. 4a). Flow surfaces are scoriaceous and reddish indicating oxidation. The volcanic edifice is characterized by the lack of pyroclastic material. It seems that the lavas were extruded over a short time as no signs of erosion or sedimentation could be found between individual flows.

4.1.2. Pleistocene volcanic activity

The three centres of Pleistocene explosive and effusive volcanism consist of basanitic lavas and pyroclastic deposits. A detailed description is given by SKJELKVÅLE et al. (1989). We present data on two of the three eruptive centers in the Bockfjord/Woodfjord area (Fig. 3): Sverrefjellet represents a composite volcano, 500 meters high and 2 km in diameter at its base. The volcanic cone has been subjected to glacial erosion. The volcanic edifice consists of subaerial and subglacial flows, fine to very coarse pyroclastic material, and radial dykes, as well as breccia vents in the central part of the volcano. Halvdanpiggen, a volcanic neck, is composed of columnar jointed lavas and explosion breccias. The vent, about 200 m in diameter, is surrounded by several radial dykes.

Abundant rounded upper mantle and lower crustal xenoliths and xenocrysts are included in the volcanic rocks of both volcanoes. They can be grouped into Cr-diopside lherzolite, wehrlite, metapyroxenite and granulite suites (AMUNDSEN et al., 1987a, 1987b). In addition, irregularly shaped upper crustal xenoliths (mica schists, marbles, migmatites and granitic rocks at Sverrefjellet; Devonian sandstones at Halvdanpiggen) occur within the lavas and pyroclastic deposits. The xenoliths (up to 30 cm in diameter) comprise 30 to 70 vol.% of the volcanic rocks.

4.2. PETROGRAPHY AND MINERAL CHEMISTRY

The nomenclature of the volcanic rocks is based on their modal and normative mineral compositions (after: YODER and TILLEY, 1962; MACDONALD and KATSURA, 1964), their chemical compositions (after: COX et al., 1979; MACDONALD and KATSURA, 1964) and nomenclature used in previous works (SKJELKVÅLE et al., 1989; HAGEN, 1988).

4.2.1. Neogene lavas

Two lava types are distinguished in the Neogene volcanic edifice on petrographical and geochemical criteria and are referred to as enriched olivine

a)

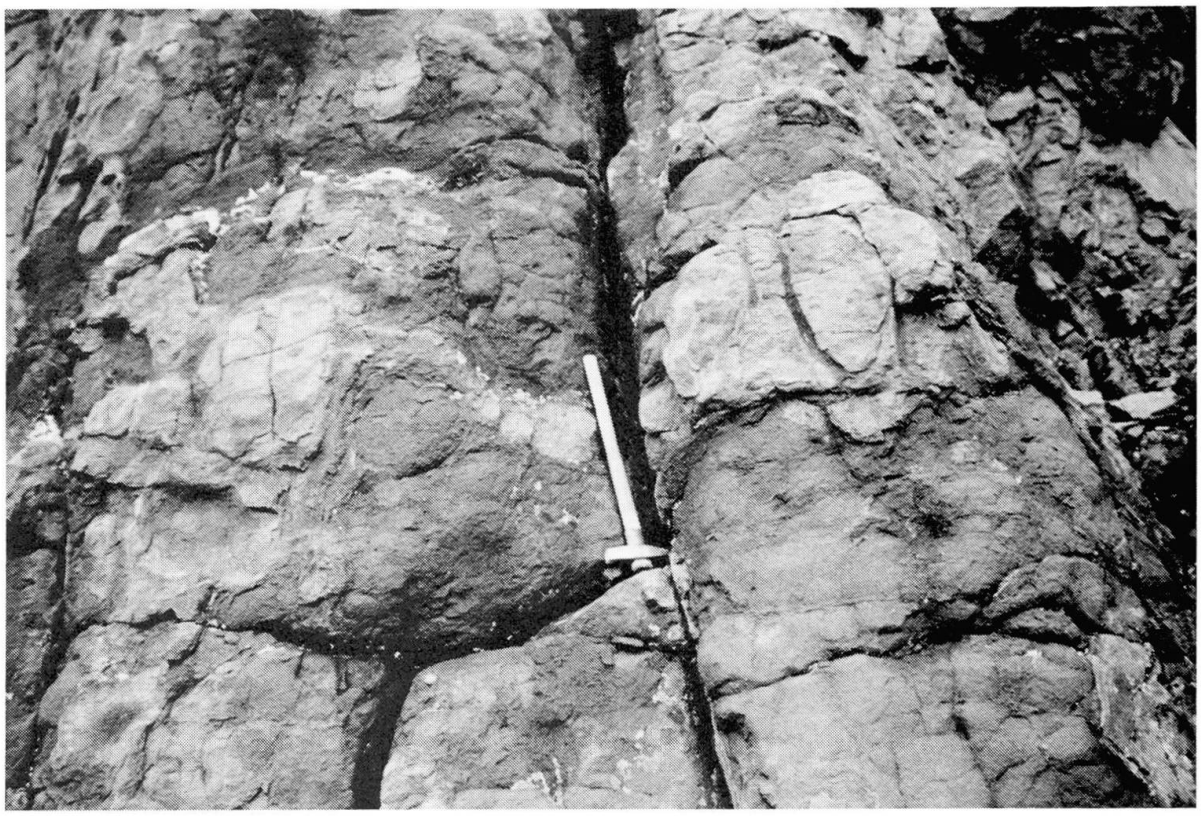

b)

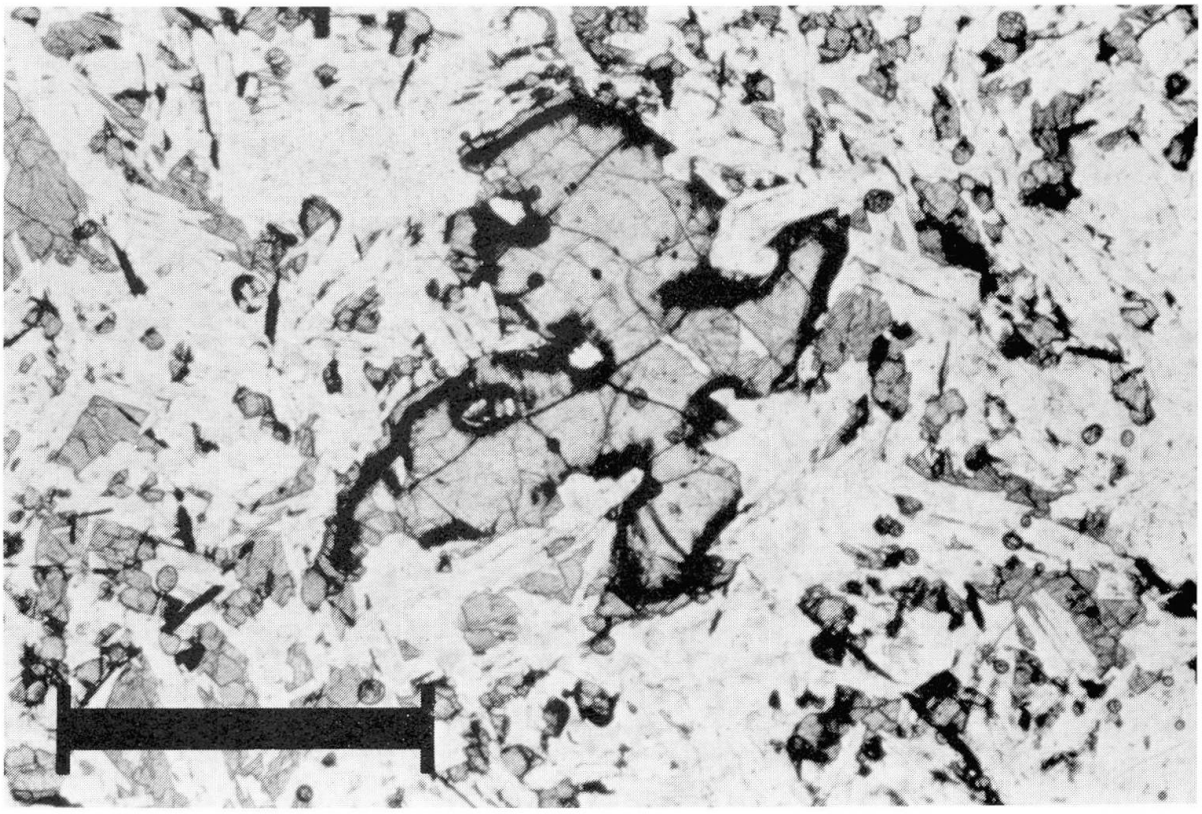

Fig. 4 a) Magma mixing structure in a Neogene lava flow at Risefjella (length of hammer: 40 cm).
b) Olivine phenocryst in a Neogene lava surrounded by an iddingsitic alteration rim which is overgrown by newly formed olivine (single polarized light, scale bar: 1 mm).

Tab. 2 Representative electron microprobe analyses of olivines from olivine tholeiites, olivine basalts and basanites from NW-Spitsbergen.

sample:	Ol-Tholeiite RF2: phenocryst..... core	rim	overgrowth	matrix	Ol-Basalt RF6: phenocryst.... core	rim	matrix	Basanite SF41: phenocryst.... core	rim	matrix
SiO2	38.95	38.12	35.30	33.86	39.57	37.47	35.07	39.90	39.57	38.77
TiO2	.01	.01	.03	.08	.00	.02	.07	.00	.00	.04
Cr2O3	.05	.08	.00	.03	.02	.04	.00	.01	.00	.00
Al2O3	.01	.05	.04	.01	.03	.05	.00	.00	.00	.01
FeO	17.57	21.69	34.91	45.18	16.80	29.07	37.45	12.97	14.83	19.23
MnO	.25	.29	.54	.67	.21	.47	.69	.19	.30	.27
MgO	42.93	39.36	28.07	19.95	42.74	32.29	26.17	46.29	44.77	41.35
NiO	.23	.19	.10	.06	.26	.12	.07	.14	.28	.14
CaO	.26	.28	.35	.37	.26	.44	.42	.19	.27	.31
Total	100.26	100.07	99.34	100.21	99.89	99.97	99.94	99.69	100.02	100.12
					CATIONS assuming stoichiometry					
Si	.9867	.9880	.9865	.9903	1.0055	1.0129	.9870	.9956	.9936	.9919
Ti	.0002	.0002	.0006	.0018	.0000	.0004	.0015	.0000	.0000	.0008
Cr	.0010	.0016	.0000	.0007	.0004	.0009	.0000	.0002	.0000	.0000
Al	.0003	.0015	.0013	.0003	.0009	.0016	.0000	.0000	.0000	.0003
Fe2	.3722	.4701	.8158	1.1051	.3570	.6572	.8815	.2707	.3114	.4114
Mn	.0054	.0064	.0128	.0166	.0045	.0108	.0164	.0040	.0064	.0059
Mg	1.6210	1.5205	1.1692	.8697	1.6188	1.3010	1.0978	1.7216	1.6756	1.5768
Ni	.0047	.0040	.0022	.0014	.0053	.0026	.0016	.0028	.0057	.0029
Ca	.0071	.0078	.0105	.0116	.0071	.0127	.0127	.0051	.0073	.0085
					ENDMEMBERS					
Forsterite	.803	.754	.578	.431	.809	.651	.543	.857	.832	.783
Fayalite	.185	.233	.404	.548	.179	.329	.436	.135	.155	.204
Tephroite	.003	.003	.006	.008	.002	.005	.008	.002	.003	.003
Monticellite	.006	.006	.006	.005	.006	.008	.007	.004	.006	.007

tholeiites and olivine basalts. Olivine basalts occur only in minor amounts within the edifice of olivine tholeiitic flows. Representative chemical analyses of the main mineral phases are given in tables 2 to 5.

a) Enriched olivine tholeiites:

The holo- to hemicrystalline, porphyritic to seriate lavas are composed of phenocrysts of olivine and plagioclase within a subophitic matrix of plagioclase, olivine, clinopyroxene, opaques and small amounts of interstitial glass. The subhedral, up to 3 mm olivine phenocrysts show normal chemical zoning from Fo_{81} to Fo_{70} and include small crystals of Cr-rich spinel. In some flows or in parts of flows the rims of olivine phenocrysts are corroded to iddingsite and overgrown by newly formed olivine (Fo_{68-58}) (Fig. 4b). Matrix olivine ranges in composition from Fo_{55} to Fo_{45}. Plagioclase phenocrysts, euhedral to anhedral, multiply twinned and up to 4 mm long, show normal zoning from An_{67} to An_{55}. Some inclusions of olivine and ilmenite are found. Matrix plagioclase laths range in composition from An_{60} to An_{45}. Some interstitial ternary feldspar is present. Augite, restricted to the matrix, occurs interstitially or as big oikocrysts (up to 3 mm). Ilmenite is present in the matrix in variable amounts. Titanomagnetites occur as inclusions in olivine and plagioclase phenocrysts, as well as in the matrix together with ilmenites.

b) Olivine basalts:

The hemicrystalline, porphyritic olivine basalts consist of olivine phenocrysts in a subophitic matrix composed of plagioclase, clinopyroxene, olivine and opaques. The mostly anhedral, up to 3 mm olivine phenocrysts with pronounced embayments show normal zoning from Fo_{81} to Fo_{65}. Inclusions of Cr-rich spinels and titanomagnetites are present. Groundmass olivines have compositions of Fo_{62} to Fo_{54}. Matrix plagioclase laths range in composition from An_{58} to An_{46}. Ternary feldspar occurs interstitially. The matrix clinopyroxenes have titanaugitic compositions (TiO_2 2.5–3.5 wt%) and occur interstitially or as oikocrysts. In contrast to the olivine tholeiites, the matrix opaques are exclusively titanomagnetites.

Tab. 3 Representative electron microprobe analyses of clinopyroxenes from olivine tholeiites, olivine basalts and basanites from NW-Spitsbergen.

sample:	Ol-Tholeiite RF2: matrix.....		Ol-Basalt RF6: matrix.....		Basanite SF41: phenocryst...		matrix.....	
	core	rim	core	rim	core	rim	core	rim
SiO2	50.81	49.22	48.04	47.12	46.42	47.36	44.31	42.34
TiO2	1.49	2.24	2.72	3.26	1.83	3.20	4.30	5.34
Cr2O3	.22	.09	.01	.00	.62	.03	.01	.03
Al2O3	2.72	2.81	4.29	5.27	5.75	5.70	8.73	9.73
Fe2O3*	.85	2.25	2.05	3.08	7.59	1.94	2.87	4.07
FeO	8.84	10.33	7.99	7.44	.00	7.41	5.59	3.54
MnO	.21	.30	.13	.12	.03	.23	.16	.06
MgO	14.25	13.03	11.82	11.98	14.10	11.44	10.55	10.71
NiO	.02	.09	.00	.02	.09	.05	.06	.05
CaO	20.19	19.28	21.77	21.36	22.75	22.19	22.45	23.00
Na2O	.38	.48	.60	.63	.75	.62	.71	.67
K2O	.00	.00	.01	.02	.01	.04	.06	.04
Total	99.97	100.11	99.43	100.30	99.94	100.21	99.80	99.58
CATIONS assuming stoichiometry and charge balance								
Si	1.8969	1.8582	1.8197	1.7710	1.7236	1.7791	1.6707	1.5990
Ti	.0418	.0636	.0775	.0921	.0511	.0904	.1219	.1517
Cr	.0065	.0027	.0003	.0000	.0182	.0009	.0003	.0009
Al	.1197	.1250	.1915	.2334	.2516	.2524	.3879	.4331
Fe3	.0238	.0638	.0583	.0872	.2121	.0549	.0813	.1156
Fe2	.2760	.3261	.2531	.2337	.0000	.2329	.1763	.1117
Mn	.0066	.0096	.0042	.0038	.0009	.0073	.0051	.0019
Mg	.7930	.7332	.6673	.6711	.7803	.6405	.5929	.6029
Ni	.0006	.0027	.0000	.0006	.0027	.0015	.0018	.0015
Ca	.8076	.7799	.8835	.8601	.9050	.8931	.9069	.9307
Na	.0275	.0351	.0441	.0459	.0540	.0452	.0519	.0491
K	.0000	.0000	.0005	.0010	.0005	.0019	.0029	.0019
ENDMEMBERS								
Wollastonite	.373	.359	.390	.362	.352	.381	.350	.341
Enstatite	.397	.368	.334	.336	.392	.321	.297	.302
Ferrosilite	.138	.163	.127	.117	.000	.116	.088	.056
Acmite	.024	.035	.045	.047	.054	.047	.055	.051
CaAl2SiO6	.013	.000	.011	.004	.000	.031	.059	.032
CaFeAlSiO6	.000	.000	.014	.040	.131	.008	.027	.065
CaCrAlSiO6	.006	.000	.000	.000	.018	.001	.000	.001
CaTiAl2O6	.042	.063	.077	.092	.051	.090	.122	.152

(*: Fe2O3 recalculated)

4.2.2. Quaternary lavas

The petrography of the Quaternary lavas is very uniform and all are classified as basanites. Only lavas from Sverrefjellet and Halvdanpiggen are described here. A detailed petrographical description of the lavas and the pyroclastic rocks is given by SKJELKVÅLE et al. (1989). Representative chemical analyses of the main mineral phases are given in tables 2 to 5.

The hemicrystalline, porphyritic lavas consist of olivine and clinopyroxene phenocrysts in a fine grained matrix of clinopyroxene, olivine, plagioclase, opaques and brown glass. Also observed are xenocrysts of olivine, clino- and orthopyroxene, spinel and amphibole, as well as xenoliths composed of these minerals. The euhedral to subhedral, up to 1 mm phenocrysts of olivine are normally zoned and range in composition from Fo_{86} to Fo_{83}. The euhedral, up to 0.5 mm clinopyroxene phenocrysts have titanaugitic composition (TiO_2 1.8–3.0 wt%). In the chemically more evolved samples some plagioclase (An_{50-40}) may occur as a phenocryst phase. Titanaugite (TiO_2 4.0–5.5 wt%), tiny crystals of olivine (Fo_{83-78}), plagioclase (An_{60-40}) and titanomagnetite form the matrix. Brown glass occurs in variable amounts usually as cryptocrystalline feldspars, clinopyroxenes and secondary minerals.

Tab. 4 Representative electron microprobe analyses of feldspars from olivine tholeiites, olivine basalts and basanites from NW-Spitsbergen.

sample:	Ol-Tholeiite RF2: phenocryst... core	rim	matrix	inter-stitial	Ol-Basalt RF6: matrix..... core	rim	inter-stitial	Basanite SF41: matrix..... core	rim
SiO2	51.05	54.03	55.58	64.62	54.19	56.61	64.45	53.07	56.73
TiO2	.05	.11	.12	.14	.13	.17	.19	.19	.80
Al2O3	30.59	28.59	27.99	21.64	28.80	26.71	21.15	29.47	27.11
FeO	.18	.56	.00	.53	.04	.41	.50	.27	.45
CaO	14.14	11.37	10.34	2.08	12.10	9.72	3.14	12.22	8.45
Na2O	3.69	4.95	5.72	8.03	4.72	5.97	7.19	4.38	5.94
K2O	.13	.29	.35	2.35	.25	.51	3.72	.36	.77
Total	99.83	99.90	100.10	99.39	100.23	100.00	100.34	99.96	100.25
CATIONS assuming stoichiometry and charge balance									
Si	2.3244	2.4451	2.4955	2.8967	2.4464	2.5448	2.8757	2.4068	2.5500
Ti	.0017	.0037	.0041	.0047	.0044	.0057	.0064	.0065	.0270
Al	1.6415	1.5249	1.4811	1.1433	1.5323	1.4151	1.1122	1.5752	1.4362
Fe3	.0069	.0212	.0000	.0199	.0015	.0154	.0187	.0102	.0169
Ca	.6898	.5513	.4974	.0999	.5853	.4682	.1501	.5938	.4069
Na	.3258	.4343	.4979	.6979	.4131	.5203	.6220	.3851	.5177
K	.0076	.0167	.0200	.1344	.0144	.0292	.2117	.0208	.0442
ENDMEMBERS									
Albite	.318	.433	.490	.749	.408	.511	.632	.385	.534
Anorthite	.674	.550	.490	.107	.578	.460	.153	.594	.420
Orthoclase	.007	.017	.020	.144	.014	.029	.215	.021	.046

A detailed study of the upper mantle xenoliths included in the basanites is given by AMUNDSEN (1987a) and AMUNDSEN et al. (1987a, 1987b). Mechanical decomposition of these xenoliths by the basanitic melts and chemical resorption of upper mantle xenocrysts (olivine, pyroxenes and spinel) has occurred, and thus, considerable chemical modification of the basanites must be expected. More detailed descriptions of the petrogenetic relationship between upper mantle xenoliths and their host-basanites will be the subject of a future investigation.

4.3. WHOLE ROCK CHEMISTRY

The chemical compositions of representative samples and their CIPW-norms are given in tables 6 to 8. Anhydrous CIPW-norms were calculated with fixed Fe_2O_3/FeO ratios of 0.10. In figure 5 some selected major element compositions of the Neogene and Pleistocene lavas are plotted; for comparison, analyses from previous works (HAGEN, 1988; PRESTVIK, 1977; SKJELKVÅLE et al., 1989) are included in these diagrams. In figure 6 incompatible element contents of representative samples are presented in chondrite-normalized spider-diagrams. Normalization values are from THOMPSON (1982) and NAKAMURA (1974).

4.3.1. Neogene lavas

As mentioned previously, there are two petrographically distinct types of Neogene lavas. This distinction is confirmed by whole rock chemistry. The subalkaline nature of the olivine tholeiites is evident in their major element compositions and normative mineral contents (Tab. 6, Fig. 5). Relatively low total alkali (3.6–4.3 wt%), moderate TiO_2 (1.2–1.3 wt%) and Al_2O_3 (15.8–17.1 wt%) contents, as well as 0–10 wt% hypersthene in their CIPW-norms are the diagnostic geochemical features. On the other hand, hygromagmatophile trace elements, such as Ba, Rb, LREE and Sr, show that these rocks are not normal but enriched tholeiites (Tab. 6 and 8, Fig. 6). This is confirmed by their chondrite-normalized $(La/Lu)_{cn}$ ratios of 3.5 to 4.5, the absence of subcalcic pyroxenes and their position relative to the "Hawaiian division line" (MACDONALD and KATSURA, 1964) defined by alkaline and subalkaline lavas in that region (Fig. 5). No Eu-anomalies are visible in the chondrite-normalized REE patterns (Fig. 6), thus, fractionation of plagioclase during the evolution of the lavas can be excluded. The small chemical variation of the olivine tholeiites seems to be controlled by olivine fractionation only. Two samples (RF10, RF14) show transitional geo-

Tab. 5 Representative electron microprobe analyses of rhombic and cubic opaques from olivine tholeiites, olivine basalts and basanites from NW-Spitsbergen.

sample:	Ol-Tholeiite RF2: matrix	matrix	Ol-Tholeiite RF2: ol-incl.	Ol-Basalt RF6: matrix	ol-incl.	ol-incl.	Basanite SF41: matrix
SiO2	.06	.18	SiO2 .11	.04	.07	.23	.08
TiO2	49.13	48.94	TiO2 1.83	26.72	24.65	13.06	25.31
Cr2O3	.04	.04	Cr2O3 29.73	.21	.10	15.44	.06
Al2O3	.00	.13	Al2O3 26.45	.85	2.35	8.33	4.28
Fe2O3*	7.14	7.12	Fe2O3* 9.11	17.36	20.51	19.84	16.74
FeO	40.65	39.93	FeO 23.28	51.67	48.51	37.37	50.44
MnO	.48	.51	MnO .00	.68	.51	.00	.71
MgO	1.62	1.79	MgO 9.37	2.33	3.30	4.65	2.82
NiO	.00	.07	NiO .08	.00	.02	.21	.04
CaO	.13	.33	CaO .00	.00	.21	.02	.05
Total	99.24	99.04	Total 99.95	99.86	100.23	99.15	100.53
CATIONS assuming stoichiometry of rhombic oxides				CATIONS assuming stoichiometry of cubic oxides			
Si	.0015	.0045	Si .0034	.0015	.0025	.0081	.0029
Ti	.9308	.9262	Ti .0427	.7381	.6690	.3448	.6808
Cr	.0008	.0008	Cr .7299	.0061	.0029	.4285	.0017
Al	.0000	.0039	Al .9680	.0368	.1000	.3446	.1804
Fe3	.1353	.1348	Fe3 .2128	.4800	.5570	.5241	.4506
Fe2	.8564	.8405	Fe2 .6044	1.5870	1.4641	1.0970	1.5087
Mn	.0102	.0109	Mn .0000	.0212	.0156	.0000	.0215
Mg	.0608	.0671	Mg .4337	.1276	.1775	.2433	.1503
Ni	.0000	.0014	Ni .0020	.0000	.0006	.0059	.0012
Ca	.0035	.0089	Ca .0000	.0000	.0081	.0008	.0019
ENDMEMBERS				ENDMEMBERS			
Hematite	.068	.068	Magnetite .058	.103	.110	.165	.104
Corundum	.000	.002	Mg-Ferrite .049	.118	.155	.099	.106
Eskolaite	.000	.000	Jacobsite .000	.020	.014	.000	.015
Ilmenite	.859	.848	Spinel .221	.009	.028	.065	.043
Geikielite	.061	.068	Hercynite .264	.008	.020	.109	.042
Mn-Ilmenite	.010	.011	Galaxite .000	.002	.002	.000	.006
			Chromite .199	.001	.001	.135	.000
			Mg-Chromite .166	.002	.001	.081	.000
(Fe2O3* recalculated)			Ulvoespinel .043	.738	.669	.345	.681

chemical features to the olivine basalts described below.

Compared to the olivine tholeiites, the olivine basalts are weakly alkaline, as shown by higher total alkali and TiO_2 contents (Tab. 6, Fig. 5). The olivine basalts have small amounts of nepheline in their norm and fall into the alkali olivine basalt group defined by GREEN and RINGWOOD (1967). Incompatible trace element contents and $(La/Lu)_{cn}$ ratios (6.0 to 6.5) are slightly higher relative to the olivine tholeiites (Tab. 6 and 8, Fig. 6). Fractionation of plagioclase can also be excluded from the REE patterns (Fig. 6).

It is not possible to relate olivine tholeiites to olivine basalts by simple crystal fractionation processes; compare degree of fractionation (Mg-numbers) and incompatible element abundances (Tab. 6 and 8, Fig. 6).

Chemical differences among mixed olivine tholeiitic lavas (samples RF1 and RF2) as well as among mixed olivine basaltic lavas (samples RF5 and RF6) are very small. This means, either mixed melts originally had similar chemical compositions, or they homogenized chemically during mixing. Because of the textural and mineral chemical disequilibria observed in these rocks, the latter explanation is more likely.

4.3.2. Quaternary lavas

Quaternary basanites have strongly alkaline, primitive to slightly evolved chemistries (Tab. 7 and 8), which are reflected in their total alkali (5.2–7.2 wt%) and MgO (18.8–11.2 wt%) contents. They are strongly nepheline-normative (12–18 wt%), strongly enriched in hygromagmatophile elements (e.g. Ba 800–1000 ppm, Sr 900–1100 ppm, La 60–100 ppm) and have steep REE patterns ($[La/Lu]_{cn}$ 20–25; Fig. 6). Olivine fractionation caused the compositional variation of the basanites shown in figure 5.

Tab. 6 Representative XRF analyses of Neogene olivine tholeiites and olivine basalts from Risefjella (detection limits of trace elements and accuracies of XRF analyses: see table 7).

type:	Ol-Tholeiites:						Ol-Basalts:	
sample	RF8	RF1	RF2	RF7	RF14	RF10	RF5	RF6
MAJOR ELEMENTS (wt%):								
SiO2	48.49	49.39	49.61	49.52	48.80	48.89	47.27	48.03
TiO2	1.45	1.32	1.31	1.26	1.33	1.15	1.60	1.64
Al2O3	17.03	15.84	16.26	15.92	15.90	15.79	15.26	15.50
Fe2O3	5.66	3.36	2.64	2.22	4.78	6.85	3.84	1.05
FeO	5.65	7.10	7.90	8.50	6.25	4.45	7.30	9.95
MnO	.17	.15	.15	.15	.16	.16	.16	.16
MgO	6.70	8.06	7.90	8.19	9.03	9.07	9.52	9.07
CaO	8.74	8.45	8.55	8.83	8.33	8.12	7.86	8.22
Na2O	3.26	3.27	3.30	3.47	3.52	3.56	3.19	3.61
K2O	.36	.68	.71	.56	.68	.77	.93	.98
P2O5	.18	.19	.17	.16	.23	.16	.28	.27
H2O+	1.81	2.12	1.23	.95	.93	.94	2.33	1.11
Total	99.50	99.93	99.73	99.73	99.94	99.91	99.54	99.59
TRACE ELEMENTS (ppm):								
F	bdl	115	21	bdl	bdl	bdl	146	bdl
Ba	177	178	185	135	180	195	230	239
Rb	bdl	4	8	bdl	4	8	8	10
Sr	313	271	302	259	348	270	389	454
Nb	bdl	bdl	bdl	bdl	bdl	bdl	9	8
Ce	bdl	21	19	bdl	bdl	bdl	26	20
Y	15	15	13	12	12	14	16	16
Zr	106	102	98	87	98	96	133	131
V	245	180	186	179	171	191	210	200
Cr	243	277	294	290	341	311	254	247
Ni	143	173	183	194	258	231	225	222
Co	61	52	52	45	66	71	58	60
Cu	58	70	68	48	62	52	61	64
Zn	92	85	85	83	88	88	89	88
Sc	26	19	21	18	20	20	20	20
Pb, Th, U, La, Nd and S below detection limit (bdl) in all samples								
ANHYDROUS CIPW NORM (wt%) with Fe2O3/FeO=0.1:								
Or	2.18	4.11	4.26	3.35	4.06	4.59	5.65	5.88
Ab	28.22	28.27	28.33	29.71	29.92	29.53	27.75	26.51
An	31.48	27.11	27.86	26.92	25.81	25.07	25.26	23.54
Ne	.00	.00	.00	.00	.08	.48	.00	2.43
Wo	4.87	6.03	5.87	6.99	6.00	6.07	5.40	6.70
Di En	2.50	3.39	3.25	3.88	3.45	3.46	3.17	3.85
Fs	2.29	2.40	2.39	2.84	2.29	2.39	1.98	2.55
Hy En	5.57	5.50	4.71	2.19	.00	.00	.00	.00
Fs	5.02	3.90	3.47	1.60	.00	.00	.00	.00
Ol Fo	6.31	8.05	8.42	10.21	13.49	13.56	14.86	13.37
Fa	6.27	6.37	6.83	8.23	9.86	10.13	10.22	9.75
Mt	1.49	1.36	1.37	1.40	1.40	1.41	1.46	1.46
Il	2.82	2.56	2.52	2.42	2.55	2.21	3.12	3.16
Ap	.43	.45	.40	.38	.54	.37	.67	.63
Mg-No.	54.59	60.57	59.74	60.10	62.28	62.25	63.07	61.63

Tab. 7 Representative XRF analyses of Pleistocene basanites from Sverrefjellet (SF) and Halvdanpiggen (HP). In the last column detection limits (d.l.) for the analyses of trace elements are listed.

locality:	Sverrefjellet:					Halvdanpiggen:	
	dyke	flow	flow	flow	tuff	vent	vent
sample:	SF33	SF25	SF15	SF4	SF14	HP9	HP18
MAJOR ELEMENTS (wt%):							
SiO2	44.99	44.81	44.92	44.83	45.21	43.92	44.11
TiO2	2.64	2.69	2.20	2.22	2.16	2.01	2.08
Al2O3	14.75	14.56	14.21	13.95	14.19	13.49	13.69
Fe2O3	2.54	2.84	2.64	2.61	2.84	4.10	4.11
FeO	7.80	7.96	7.41	7.33	7.05	6.15	6.28
MnO	.15	.16	.15	.15	.15	.16	.16
MgO	8.76	9.09	9.76	10.52	10.13	11.17	10.81
CaO	8.35	8.38	8.93	8.91	8.92	7.97	8.28
Na2O	4.72	4.86	4.78	4.38	4.63	4.30	4.57
K2O	2.20	2.31	2.02	1.98	2.10	1.91	2.00
P2O5	.78	.76	.88	.86	.87	.86	.86
H2O+	1.42	1.02	1.33	1.59	1.12	1.49	1.55
Total	99.09	99.44	99.23	99.33	99.37	97.53	98.50
TRACE ELEMENTS (ppm):							(d.l.)
F	788	484	475	497	431	271	272 (10)
Ba	804	806	917	962	869	881	945 (3)
Rb	42	43	39	40	42	39	43 (4)
Sr	940	937	1011	1028	1012	1085	1093 (4)
Pb	bdl	bdl	bdl	bdl	bdl	bdl	bdl (6)
Th	bdl	bdl	bdl	bdl	bdl	bdl	bdl (6)
U	bdl	bdl	bdl	bdl	bdl	bdl	bdl (10)
Nb	60	62	59	59	61	55	59 (3)
La	58	60	58	59	62	54	61 (12)
Ce	90	99	107	110	114	121	122 (23)
Nd	37	43	40	42	43	42	40 (12)
Y	17	21	19	20	18	18	19 (4)
Zr	239	246	223	219	224	210	210 (4)
V	233	243	213	202	188	189	180 (3)
Cr	207	234	354	359	352	417	392 (10)
Ni	173	191	259	277	267	339	306 (7)
Co	67	74	81	60	52	56	65 (6)
Cu	23	19	23	27	34	27	30 (7)
Zn	102	104	98	92	97	96	93 (5)
Sc	13	14	14	12	12	12	12 (1)
S	bdl	73	119	77	150	bdl	107 (16)
ANHYDROUS CIPW NORM (wt%) with Fe2O3/FeO = 0.1:							
Or	13.30	13.86	12.18	11.96	12.62	11.74	12.18
Ab	11.24	8.52	9.23	9.65	9.21	10.89	8.92
An	12.85	11.26	11.59	12.83	11.93	12.34	11.27
Ne	16.05	18.01	17.36	15.30	16.59	14.61	16.75
Wo	10.15	10.82	11.59	11.11	11.39	9.58	10.55
Di En	6.19	6.57	7.24	7.11	7.23	6.15	6.70
Fs	3.40	3.66	3.65	3.27	3.44	2.80	3.18
Ol Fo	11.31	11.51	12.31	13.79	12.92	15.98	14.75
Fa	6.85	7.07	6.83	6.98	6.78	8.01	7.71
Mt	1.36	1.41	1.32	1.30	1.29	1.35	1.35
Il	5.13	5.19	4.26	4.31	4.17	3.97	4.07
Ap	1.85	1.79	2.08	2.04	2.05	2.07	2.05
Mg-No	62.63	62.51	65.79	67.70	67.03	68.63	67.61

Tab. 8 Representative INA analyses of Neogene lavas from Risefjella (RF) and ICP-MS analyses of Pleistocene volcanics from Sverrefjellet (SF) and Halvdanpiggen (HP). Estimated absolute accuracies (1 σ) of the analyses are given for samples RF10 (INAA) and HP9 (ICP-MS).

type:	Ol-Tholeiites:							Ol-Basalts:		Basanites:			
sample:	RF8	RF1	RF2	RF7	RF14	RF10	(±1σ)	RF5	RF6	SF25	SF4	HP9	(± 1σ)
La	11.3	12.3	12.6	9.51	12.3	12.3	(± 0.3)	16.6	17.2	52.4	71.0	75.2	(± 1.0)
Ce	24.1	26.6	25.1	21.0	24.8	26.8	(± 0.3)	34.2	33.9	89.9	109	114	(± 1)
Pr	na	na	na	na	na	na		na	na	11.1	12.2	12.7	(± 0.1)
Nd	13.8	13.7	13.2	11.7	12.3	12.9	(± 0.3)	16.6	17.6	53.3	53.4	56.3	(± 1.0)
Sm	3.78	3.66	3.58	3.27	3.33	3.42	(± 0.03)	4.38	4.40	9.08	8.80	8.89	(± 0.08)
Eu	1.35	1.26	1.21	1.17	1.25	1.20	(± 0.01)	1.46	1.47	3.19	3.00	3.08	(± 0.03)
Tb	0.62	0.59	0.52	0.57	0.50	0.60	(± 0.03)	0.59	0.63	1.34	1.28	1.26	(± 0.01)
Dy	na	na	na	na	na	na		na	na	6.24	5.94	6.00	(± 0.05)
Ho	na	na	na	na	na	na		na	na	1.03	1.04	1.04	(± 0.01)
Er	na	na	na	na	na	na		na	na	2.88	2.89	2.93	(± 0.03)
Tm	na	na	na	na	na	na		na	na	0.31	0.32	0.33	(± 0.01)
Yb	2.12	1.97	1.83	1.97	1.62	1.95	(± 0.09)	1.83	1.97	1.91	2.03	2.04	(± 0.06)
Lu	0.32	0.30	0.30	0.30	0.28	0.28	(± 0.02)	0.29	0.27	0.27	0.29	0.31	(± 0.01)
Th	1.41	1.79	1.72	1.11	1.42	1.95	(± 0.08)	2.12	2.01	na	na	na	
U	0.06	0.12	0.36	0.10	0.31	0.37	(± 0.07)	0.40	0.10	1.94	2.41	2.36	(± 0.10)
Hf	2.89	2.65	2.48	2.36	2.45	2.56	(± 0.04)	3.19	3.34	6.85	6.16	5.69	(± 0.15)

5. Discussion

In NW-Spitsbergen two types of volcanism occurred in the same area within a short time period:

1. Extensive Neogene volcanism yielded voluminous plateau lavas. The petrography and the chemical characteristics of these slightly differentiated lavas are transitional from tholeiitic to alkaline.

2. Relative to the voluminous Neogene volcanism, only small amounts of strongly alkaline volcanic rocks form the Pleistocene volcanoes. These primitive to slightly differentiated basanites are very rich in xenolithic material from the upper mantle and the lower crust.

The petrologic evolution of the Neogene olivine tholeiitic lavas was dominated by low-pressure crystallization. This is evident from the phenocryst assemblage of olivine and plagioclase, indicating a crystallization depth of less than 15 km (GREEN and RINGWOOD, 1967). Geochemical considerations (e.g. REE patterns), however, suggest that olivine was the only fractionating phase during the evolution of the lavas from their parental, probably picritic melts with low incompatible element contents. In the case of the Neogene olivine basalts, fractionation of olivine from picritic melts, slightly enriched in incompatible elements relative to parental melts of the olivine tholeiites, and only minor low-pressure crystallization is proposed. Petrological data on the Neogene lavas suggest crystallization and mixing of mantle-derived, subalkaline to weakly alkaline melt batches in upper crustal magma chambers. This is consistent with models for the evolution of Neogene lavas at Okstindane mountain (Woodfjord area, NW-Spitsbergen) by HAGEN (1988). If the olivine phenocrysts and Cr-spinel inclusions in olivines are considered to be liquidus phases in the olivine tholeiites and olivine basalts, it is likely that they originated in the upper mantle at depth less than approximately 40 to 50 km (GREEN and RINGWOOD, 1967; ELTHON and SCARFE, 1984). The garnet-/spinel-lherzolite transition below Spitsbergen is determined to be situated at depths of approximately 60 km (AMUNDSEN, 1987b). Therefore, it is very likely the Neogene lavas on Spitsbergen originated in the spinel-lherzolitic part of the upper mantle.

In contrast, the Pleistocene basanites were dominated by higher pressure crystallization, indicated by their phenocryst assemblage of olivine and titanaugite; experimental studies on alkali olivine basalts and basanites (GREEN and RINGWOOD, 1967; TAKAHASHI, 1980) suggest pressures of 10 to 15 kb for this liquidus phase assemblage. The primitive, strongly alkaline chemical characteristics of our samples suggest small amounts of olivine fractionation from a primary melt composition enriched in incompatible elements. The occurrence of mantle xenoliths within the basanites indicates rapid ascent of these lavas from the upper mantle. According to AMUNDSEN et al. (1987a, 1987b), the predominant xenolith types from the upper mantle (spinel lherzolites and pyroxenites) equilibrated between 10 and 15 kb, giving a minimum depth of approximately 50 km for basanitic melt generation. Therefore, it is not clear whether

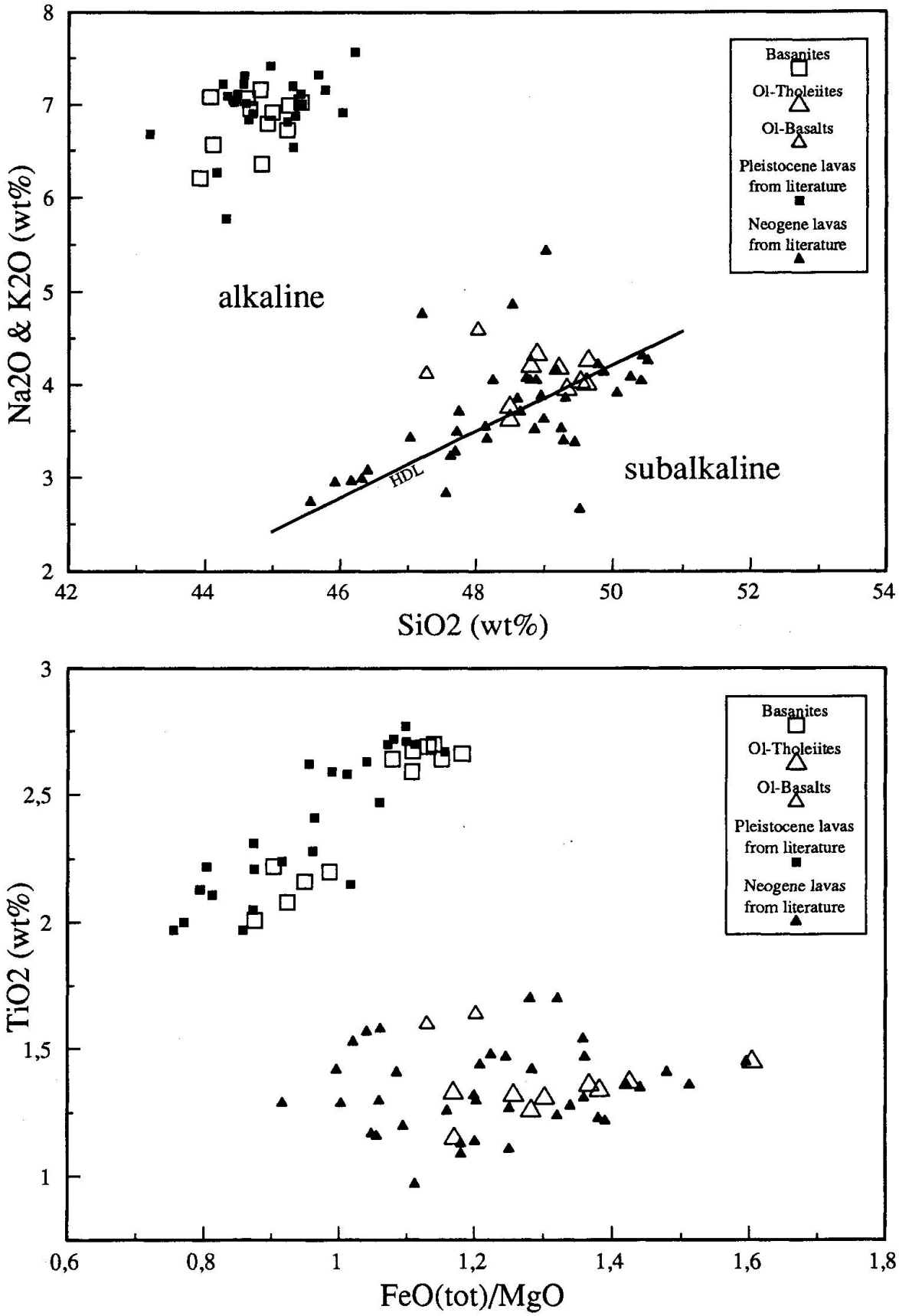

Fig 5 Graphical representations of geochemical analyses of Neogene olivine basalts and olivine tholeiites and Pleistocene basanites from NW-Spitsbergen, supplemented by data from literature (Neogene lavas: PRESTVIK, 1977; HAGEN, 1988; Pleistocene lavas: SKJELKVÅLE et al., 1989). HDL: "Hawaiian Division Line" of alkaline and subalkaline lavas on Hawaii (MACDONALD and KATSURA, 1964).

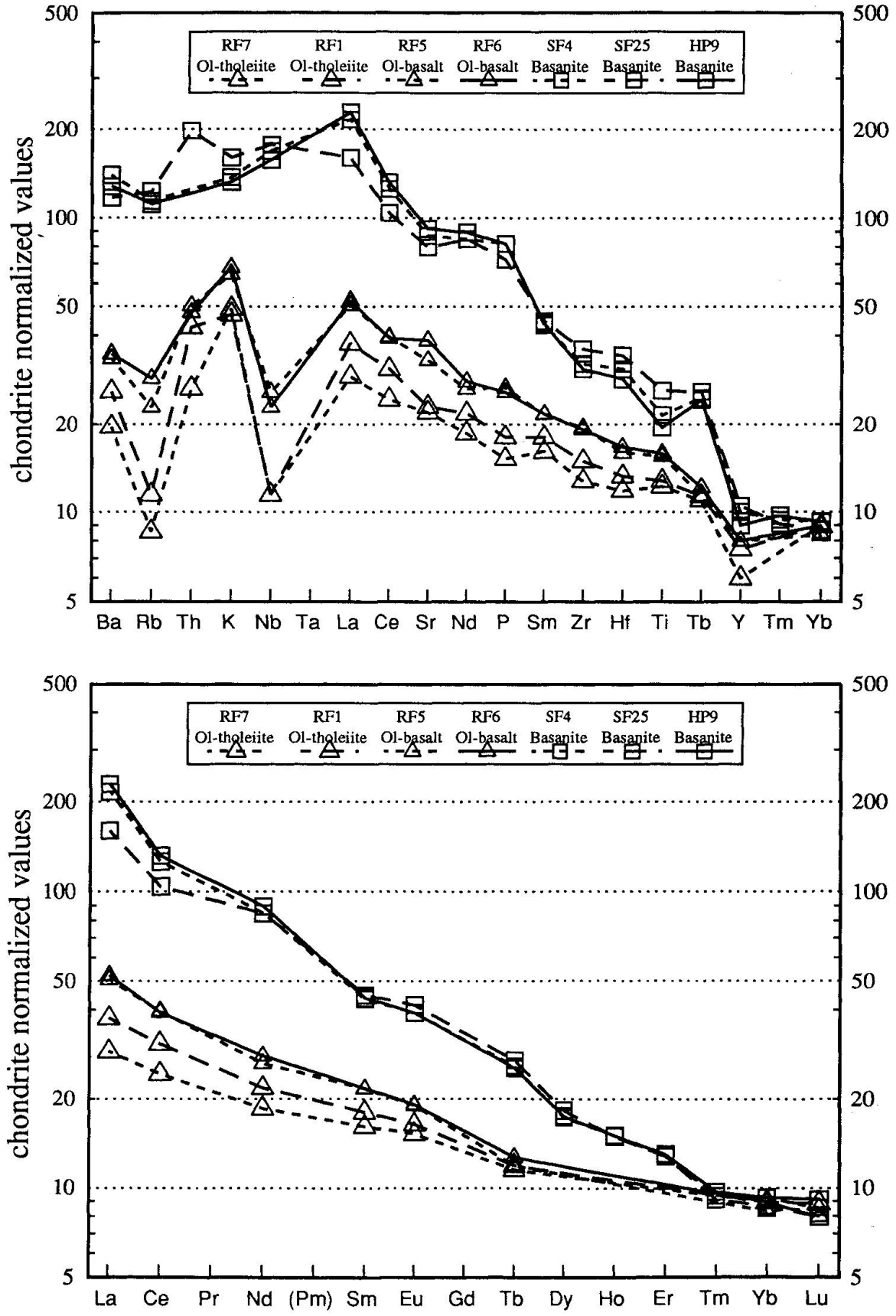

Fig. 6 Chondrite normalized spider diagrams of incompatible and rare earth elements (normalization values: NAKAMURA, 1974; THOMPSON, 1982) from selected Neogene olivine basalts and olivine tholeiites and Pleistocene basanites from NW-Spitsbergen.

the Pleistocene basanites were derived from garnet- or spinel-lherzolitic mantle below Spitsbergen.

On the other hand, bulk chemistries of Pleistocene basanitic and Neogene olivine tholeiitic/basaltic magmas require mantle sources with different degrees of enrichment in highly incompatible elements, such as LREE, Ba, Th and U. Relative incompatible element contents, especially REE patterns, are consistent with a garnet-bearing residue for the Pleistocene and a spinel-bearing residue for the Miocene partial melts. FURNES et al. (1986) grouped the spinel-lherzolitic mantle xenoliths in the basanites from NW-Spitsbergen into less refractory and more refractory types, based on their modal mineral and compatible element contents. Relative concentrations of specific highly incompatible elements (La, Th, U, K) do not strictly follow this distinction, because some of the most refractory samples have the highest abundances of these elements (FURNES et al., 1986). This means the spinel-lherzolitic part of the upper mantle below Spitsbergen suffered at least one partial melting and basalt extraction event, accompanied or followed by metasomatism. Similar depletion processes and cryptic as well as modal metasomatism of spinel-lherzolites from NW-Spitsbergen are discussed in more detail by AMUNDSEN (1987a). Preliminary results of Nd- and Sr-isotope analyses of the described lava types show that the Pleistocene basanites were generated from a depleted mantle source (high positive ε_{Nd}, high negative ε_{Sr}), whereas the Neogene olivine tholeiites and olivine basalts are generated from an inhomogeneous, relatively undepleted mantle source (variably low positive ε_{Nd}, variably low ε_{Sr}). This difference precludes the possibility, that the Neogene and Pleistocene lavas in NW-Spitsbergen are derived from the same mantle source by different degrees of partial melting.

Considering the petrological arguments presented above, we assume a depleted, garnet-lherzolitic mantle at depths more than 60 km as the source of the Pleistocene basanitic melts, while the Neogene olivine-tholeiitic/basaltic lavas originated in an inhomogeneous, relatively undepleted spinel-lherzolitic mantle at depths less than 60 km. The apparent contradiction of isotope and trace element chemistries within basanitic and within olivine tholeiitic/basaltic melts may be explained by different degrees of partial melting in their upper mantle sources: a low degree of partial melting in the garnet-lherzolitic source and a high degree of partial melting in the spinel-lherzolitic source. The ultramafic xenoliths incorporated in the Pleistocene basanites are recording Neogene basalt extraction and metasomatism in the lithosphere below Spitsbergen. The variability of isotope and trace element chemistries of Neogene lavas may be explained by contamination of the spinel-lherzolitic mantle with basanitic melts derived from the garnet-lherzolitic mantle below.

The Neogene lavas erupted onto a Late Tertary peneplain now exposed at elevations of 800 to 1200 meters above sea level (Fig. 3). In contrast, the Pleistocene volcanic edifices occur in different topographic regions of the present-day relief (Fig. 3). The time span between the Neogene and the Pleistocene volcanic episode is approximately 10 m.y. This places a magnitude of uplift of several 100 meters after the extrusion of the Neogene lavas with an averaged uplift rate of about 0.1 mm per year during the last 10 m.y. The timing of uplift is consistent with geophysical evidence for a reactivation of the pre-Oligocene Yermak Hot Spot since Miocene times: Geomagnetic and bathymetric data indicate an increase of igneous activity since magnetic anomaly 5 (approximately 10 m.y.) at the southern end of the Nansen ridge (Yermak H-zone, FEDEN et al., 1979). After CRANE et al. (1982) the westernmost part of the Yermak Plateau is not of pre-Oligocene age but was formed later than magnetic anomaly 7 (approximately 13 m.y.). They relate the igneous activity forming the westernmost Yermak Plateau to a readjustment and migration of the oblique Spitsbergen Transform Zone which tends to approach an orthogonal transform-ridge configuration.

The onset of continental volcanism on Spitsbergen is coeval with the onset of increased magmatic activity on the Yermak Plateau and at the southern end of the Nansen Ridge. Increased Late Cenozoic magmatic activity in this region (on-shore and off-shore) is restricted to an area of approximately 500 km in diameter and suggests a local thermal mantle-anomaly below this area. This idea is supported by the raised geothermal gradient of the lithosphere below Spitsbergen (AMUNDSEN et al., 1987a, 1987b). The extrusion of voluminous tholeiitic lavas generated at shallow depths in the upper mantle prior to the extrusion of small amounts of strongly alkaline basanites generated in deeper parts of the upper mantle, may both be explained by the model of deep mantle plumes proposed by RICHARDS et al. (1989). Therefore, magmatic characteristics of Late Cenozoic volcanism in Spitsbergen give further evidence for a revival of the pre-Oligocene Yermak Hot Spot since the Miocene.

6. Conclusions

The petrologic characteristics of Neogene and Pleistocene volcanism in NW-Spitsbergen presented in this study, together with the tectonic evolution of Svalbard and adjacent regions in late Cenozoic times and geophysical data, allow a scenario for the tectono-magmatic evolution of Spitsbergen since the Miocene to be proposed: A rising deep mantle plume in the area between Svalbard and Greenland induced extensive partial melting and metasomatism in the lithospheric mantle. Ascending melts, with lithospheric and deep mantle source characteristics, were trapped in magma chambers within the crust. After fractional crystallization and mixing processes, the extrusion of olivine tholeiitic and olivine basaltic magmas gave rise to the formation of an extended lava plateau on northwestern Spitsbergen. Subsequent strong uplift of Svalbard is an expression of the rising mantle plume. The Quaternary volcanoes are composed of deep mantle melts, which incorporated and transported large amounts of metasamotized lithospheric xenoliths to the surface.

Acknowledgements

Our thank is owed to H.E.F. Amundsen (Oslo) who supported this study by stimulating discussions and provided the isotope chemical analyses. We are greatly indepted to the Swiss Alpine Club of Zürich, particularly to H. Schlegel and the other participants of the expedition for their logistical support of our field work. Thanks to Y. Ohta and the Polar Research Institute (Oslo) for their conciliating support. We thank L. Tobler (PSI, Würenlingen) for helping with INA analyses and P. Richner (EMPA, Dübendorf) for supporting us with ICP-MS analytics. A travel grant by the Swiss Federal Institute of Technology in Zürich is gratefully acknowledged. We appreciated the critical and constructive discussions with V. Dietrich, P. Ulmer and R. Sweeney who helped to improve the manuscript. Thanks to H.E.F. Amundsen for his critical and careful review and to G. Früh-Green for helping with the English.

References

Amundsen, H.E.F. (1987a): The lithosphere beneath northwestern Spitsbergen: evidence from upper mantle and lower crustal xenoliths. Unpubl. Cand. Scient. Thesis, Univ. of Oslo, 128 pp.

Amundsen, H.E.F. (1987b): Evidence for liquid immiscibility in the upper mantle. Nature, 327, 692–695.

Amundsen, H.E.F., Griffin, W.L. and O'Reilly, S.Y. (1987a): The lower crust and upper mantle beneath northwestern Spitsbergen: evidence from xenoliths and geophysics. Tectonophysics, 139, 169–185.

Amundsen, H.E.F., Griffin, W.L. and O'Reilly, S.Y. (1987b): The nature of the lithosphere beneath northwestern Spitsbergen: xenolith evidence. Nor. geol. unders. Special Publ., 3, 58–65.

Ayranci, B. (1977): The major-, minor-, and trace-element analysis of silicate rocks and minerals from a single sample solution. Schweiz. Mineral. Petrogr. Mitt., 57, 299–312.

Birkenmajer, K. (1981): The geology of Svalbard, the western part of the Barents Sea and the continental margin of Scandinavia. In: Nairn, A.E.M., Churkin, M. & Stehli, F.C. (eds). The Ocean Basins and Margins (Vol. 5, The Arctic Ocean). Plenum Press, New York, 265–329.

Cox, K.G., Bell, J.D. and Pankhurst, R.J. (1979): The interpretation of igneous rocks. Allen and Unwin, London, 450 pp.

Crane, K., Eldholm, O., Myhre, A.M. and Sundvor, E. (1982): Thermal implications for the evolution of the Spitsbergen transform fault. Tectonophysics, 89, 1–32.

Dietrich, V., Oberhänsli, R. and Walpen, P. (1976): Röntgenfluoreszenzanalyse der Silikatgesteine (internal report): Zürich (Inst. f. Kristall. u. Petrogr. der ETH Zürich), 65 pp.

Dickin, A.P. (1988): The North Atlantic Tertiary Province. In: Mac Dougall, J.D. (ed.). Continental Flood Basalts. Kluwer Academic Publishers, Dordrecht, 111–149.

Eldholm, O. and Talwani, M. (1977): Sediment distribution and structural framework of the Barents Sea. Geol. Soc. Am. Bull., 88, 1015–1029.

Elthon, D. and Scarfe, C.M. (1984): High-pressure phase equilibria of a high-magnesia basalt and the genesis of primary oceanic basalts. Am. Mineral., 69, 1–15.

Feden, R.H., Vogt, P.R. and Fleming, H.S. (1979): Magnetic and bathymetric evidence for the "Yermak" hot spot northwest of Svalbard in the Arctic Basin. Earth Planet. Sci. Lett., 44, 18–38.

Friend, P.F. and Moody-Stuart, M. (1972): Sedimentation of the Wood Bay Formation (Devonian) of Spitsbergen: Regional analysis of a late orogenic basin. Norsk Polarinstitutt Skrifter, 157, 77 pp.

Furnes, H., Pedersen, R.B. and Maaløe, S. (1986): Petrology and geochemistry of spinel peridotite nodules and host basalt, Vestspitsbergen. Norsk Geologisk Tidsskrift, 66, 53–68.

Gayer, R.A., Gee, D.G., Harland, W.B., Miller, J.A., Spall, H.R., Wallis, R.H. and Wisnes, T.S. (1966): Radiometric age determinations on rocks from Spitsbergen. Norsk Polarinstitutt Skrifter, 137, 1–39.

Gee, D.G. and A. Hjelle, A. (1966): On the crystalline rocks of north-west Spitsbergen. Norsk Polarinstitutt Årbok 1964, 31–45.

Gjelsvik, T. (1963): Remarks on the structure and composition of the Sverrefjellet volcano, Bockfjorden, Vestspitsbergen. Norsk Polarinstitutt Årbok 1962, 50–54.

Gjelsvik, T. (1979): The Hecla Hoek ridge of the Devonian Graben between Liefdefjorden and Holtedahlfonna, Spitsbergen. Norsk Polarinstitutt Skrifter, 167, 63–71.

Green, D.H. and Ringwood, A.E. (1967): The genesis of basaltic magmas. Contr. Mineral. and Petrol., 15, 103–190.

Hagen, H. (1988): Modelling of chemical processes in magma chambers: the evolution of a Tertiary olivine tholeiite sequence from Okstindane, NW Spitsber-

gen. Unpubl. Cand. Scient. Thesis, Univ. of Oslo, 90 pp.

HANISCH, J. (1984): West Spitsbergen Fold Belt and Cretaceous opening of the Northeast Atlantic. In: Spencer, A.M. et al. (eds). Petroleum Geology of the North European Margin. Graham & Trotman, London, 187–198.

HARLAND, W.B. (1969): Contribution of Spitsbergen to understanding of tectonic evolution of North Atlantic region. Mem. Am. Assoc. Petrol. Geol., 12, 817–851.

HARLAND, W.B., CUTBILL, J.L., FRIEND, P.F. GOBBETT, D.J., HOLLIDAY, D.W., MATON, P.I., PARKER, J.R. and WALLIS, R.H. (1974): The Billefjorden Fault Zone, Spitsbergen – the long history of a major tectonic lineament. Norsk Polarinstitutt Skrifter, 161, 72 pp.

HJELLE, A. (1966): The composition of some granitic rocks from Svalbard. Norsk Polarinstitutt Årbok 1965, 7–30.

HJELLE, A. and LAURITZEN, Ø. (1982): Geological map of Svalbard, 1 : 500 000, Sheet 3G, Spitsbergen northern part. Norsk Polarinstitutt Skrifter, 154C, 15 pp.

HJELLE, A. and OHTA, Y. (1974): Contribution to the geology of north western Spitsbergen. Norsk Polarinstitutt Skrifter, 158, 1–107.

HOEL, A. (1914): Nouvelles observations sur le district volcanique du Spitsberg du nord. Vid. Selk. Skr. (Kristiania), Mat. Nat. kl. 1/9.

HOEL, A. and HOLTEDAHL, O. (1911): Les nappes de lave, les volcans et les sources thermales dans les environs de la Baie Wood au Spitsberg. Vid. Selsk. Skr. (Kristiania), Mat. Nat. kl., 1/8.

JACKSON, H.R., JOHNSON, G.L., SUNDVOR, E. and MYHRE, A.M. (1984): The Yermak Plateau: formed at a triple junction. J. Geophys. Res., 89, 3223–3232.

KRISTOFFERSON, Y. and TALWANI, M. (1977): Extinct triple junction south of Greenland and the Tertiary motion of Greenland relative to North America. Geol. Soc. Am. Bull., 88, 1037–1049.

LAMAR, D.L., REED, W.E. and DOUGLASS, D.N. (1986): Billefjorden fault zone, Spitsbergen: Is it part of a major Late Devonian transform? Geol. Soc. Am. Bull., 97, 1083–1088.

MACDONALD, G.A. and KATSURA, T. (1964): Chemical Composition of Hawaiian Lavas. J. Petrol., 5/1, 82–133.

NAKAMURA, N. (1974): Determination of REE, Ba, Fe, Mg, Na and K in carbonaceous and ordinary chondrites. Geochim. Cosmochim. Acta, 38, 757–775.

NISBET, E.G., DIETRICH, V.J. and ESENWEIN, A. (1979): Routine trace element determination in silicate minerals and rocks by X-ray fluorescence. Fortschr. Miner., 57, 264–279.

PRESTVIK, T. (1977): Cenozoic plateau lavas of Spitsbergen – a geochemical study. Norsk Polarinstitutt Årbok 1977, 129–143.

REUSSER, E. (1987): Phasenbeziehungen im Tonalit der Bergeller Intrusion (Graubünden, Schweiz / Provinz Sondrio, Italien). Ph. D. thesis, no. 8329, ETH Zürich, 220 pp.

RICHARDS, M.A., DUNCAN, R.A. and COURTILLOT, V.E. (1989): Flood Basalts and Hot-Spot Tracks: Plume Heads and Tails. Science, 246, 103–107.

SALVIGSEN, O. and ÖSTERHOLM, H. (1982): Radiocarbon dated raised beaches and glacial history of the northern Spitsbergen Coast, Svalbard. Polar Research, 1, 97–105.

SCHUBIGER, P.A., PATRY, J. and WYTTENBACH, A. (1978): JANE II – Ein Vielzweckprogramm zur quantitativen Auswertung von γ-Spektren. Internal report EIR – Bericht 345, Würenlingen, 66 pp.

SKJELKVÅLE, B.-L., AMUNDSEN, H.E.F., O'REILLY, S.Y., GRIFFIN, W.L. and GJELSVIK, T. (1989): A primitive alkali basaltic stratovolcano and associated eruptive centers, northwestern Spitsbergen: volcanology and tectonic significance. J. Volcanol. Geotherm. Res., 37, 1–19.

STEEL, R.J. and WORSLEY, D. (1984): Svalbard's post-Caledonian strata – an atlas of sedimentational patterns and palaeogeographic evolution. In: Spencer, A.M. et al. (eds). Petroleum Geology of the North European Margin. Graham & Trotman, London, 109–135.

TAKAHASHI, E. (1980): Melting relations of an alkali-olivine basalt to 30 kbar and their bearing on the origin of alkali basalt magmas. Yb. Carnegie Instn., Wash., 79, 271–276.

TALWANI, M. and ELDHOLM, O. (1977): Evolution of the Norwegian-Greenland Sea. Geol. Soc. Am. Bull., 88, 969–999.

THOMPSON, R.N. (1982): Magmatism of the British Tertiary Volcanic Province. Scott. J. Geol., 18, 49–107.

VOGT, P.R., KOVACS, L.C., BERNERO, C. and SRIVASTAVA, S.P. (1982): Asymmetric geophysical signatures in the Greenland-Norwegian and southern Labrador seas and the Eurasia Basin. In: JOHNSON, G.L. and SWEENEY, J.F. (Ed.): Structure of the Arctic. Tectonophysics, 89, 95–160.

WEIGAND, P.W. and TESTA, S.M. (1982): Petrology and geochemistry of Mesozoic dolerites from the Hinlopenstretet area, Svalbard. Polar Research, 1, 35–52.

WYTTENBACH, A., BAJO, S. and TOBLER, L. (1983): Group Separation of Rare Earth Elements by Liquid-Liquid Extraction for the Neutron Activation Analysis of Silicate Rocks. Journal of Radioanalytical Chemistry, 78, 283–294.

YODER, H.S. and TILLEY, C.E. (1962): Origin of Basalt Magmas: An Experimental Study of Natural and Synthetic Rock Systems. J. Petrol., 3, 342–532.

Manuscript received Janury 15, 1992; revised manuscript accepted May 8, 1992.